The Journal of Physiology

Excessive training does not induce mitochondrial dysfunction or impair insulin signalling within skeletal muscle

Geneviève J. DesOrmeaux[1], Henver S. Brunetta[1], Pierre-Andre Barbeau[1], Alexandra M. Coates[1,2], Christopher Pignanelli[1], Fasih A. Rahman[1], Jamie F. Burr[1] and Graham P. Holloway[1]

[1]*Department of Human Health Sciences, College of Biological Sciences, University of Guelph, Guelph, Ontario, Canada*
[2]*Exercise Physiology and Performance Laboratory, Department of Biomedical Physiology and Kinesiology, Simon Fraser University, Burnaby, British Columbia, Canada*

Handling Editors: Paul Greenhaff & Russell Hepple

The peer review history is available in the Supporting Information section of this article (https://doi.org/10.1113/JP289538#support-information-section).

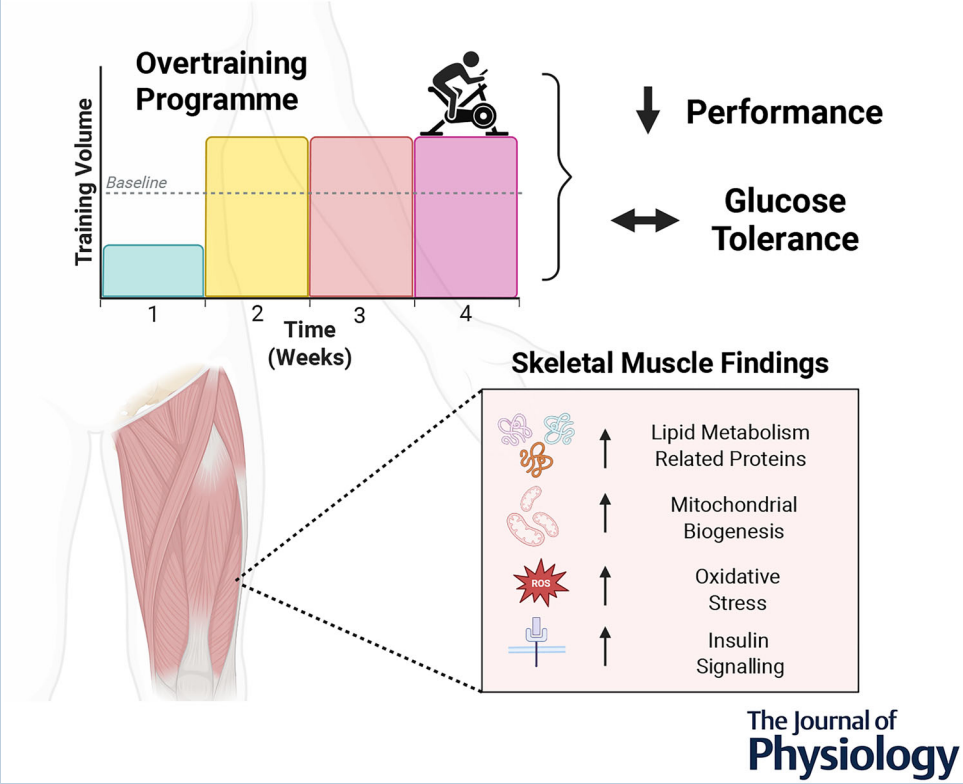

Abstract figure legend Three weeks of overtraining in trained endurance athletes reduced exercise performance without impairing glucose tolerance. In skeletal muscle, overtraining was associated with increased expression of lipid metabolism-related proteins, enhanced mitochondrial biogenesis and preserved insulin signalling, despite elevated oxidative stress. Combined, these data indicate that excessive training does not induce mitochondrial dysfunction or insulin resistance in skeletal muscle.

G. J. DesOrmeaux & H. S. Brunetta have shared first authorship.

 DOI: 10.1113/JP289538

Abstract Excessive training, also known as overtraining, has been suggested to impair skeletal muscle mitochondrial function and glucose homeostasis, challenging the notion that exercise is inherently beneficial. However, methodological limitations on assessment of mitochondrial bioenergetics while considering exercise-induced mitochondrial biogenesis make the metabolic consequences of overtraining still debatable. Therefore, we investigated skeletal muscle insulin signalling and mitochondrial bioenergetics in skeletal muscle following a 3-week overtraining protocol in healthy highly trained endurance athletes. Proteomics of skeletal muscle revealed an upregulation of proteins related to fatty acid metabolism and mitochondrial content induced by overload training. Functionally, mitochondrial respiratory capacity as well as H_2O_2 emission were increased in permeabilized muscle fibres. These effects were dependent on mitochondrial content, suggesting preservation of intrinsic mitochondrial oxidative phosphorylation. While sub-maximal mitochondrial H_2O_2 emission and oxidative stress were increased following excessive training, insulin signalling within skeletal muscle (i.e., Akt phosphorylation) during an oral glucose challenge was improved, suggesting excessive exercise does not induce skeletal muscle insulin resistance. In a further analysis, based on their psycho-physiological performances, participants were identified by who successfully or not developed an overreaching phenotype. This approach revealed a unique proteome signature in individuals who were overreached, marked by a smaller increase in proteins involved in cytoskeleton organization, glycogen metabolism, and protein translation. However, despite such classification, we did not observe reductions in either mitochondrial bioenergetics or insulin signalling within skeletal muscle. Altogether, overtraining in highly active individuals induces mitochondrial biogenesis without impairments in skeletal muscle insulin signalling nor mitochondrial oxidative capacity.

(Received 19 June 2025; accepted after revision 13 May 2026; first published online 10 June 2026)
Corresponding authors G. J. DesOrmeaux, H. S. Brunetta and G. P. Holloway: Animal Science and Nutrition Building, University of Guelph, 50 Stone Road East, N1G 2W1, Ontario, Canada. Email: gdesorme@uoguelph.ca; hbrunett@uoguelph.ca; ghollowa@uoguelph.ca

Key points

- Proteomics revealed upregulation of fatty acid and mitochondrial proteins by excessive training.
- Overtraining does not cause mitochondrial dysfunction.
- Improved insulin signalling in skeletal muscle post-overtraining.
- Overreached athletes show blunted increase in protein synthesis and metabolism.

Introduction

Mitochondrial adaptations across the movement spectrum are synonymous with health. While a cornerstone of exercise adaptions is the ability of training to stimulate mitochondrial biogenesis through the coordination of nuclear and mitochondrial genomes (Holloszy, 1967), exercise training also enhances mitochondrial respiration, supercomplex formation, density of cristae, and morphology (Axelrod et al., 2019;

Geneviève J. DesOrmeaux completed her MSc under the supervision of Dr. Graham Holloway at the University of Guelph, Canada where she is currently persuing her PhD under the same supervision. Her research focuses on the effects of physical (in)activity and dietary modulation on mitochondrial bioenergetics and related physiological parameters in skeletal muscle. **Henver S. Brunetta** has a PhD from the Federal UNiversity of Santa Catarine (Brazil) under the supervision of Dr. Everson Nunes in the Department of Physiological Sciences. During his post-doctoral training, he worked at the University of Guelph under the supervision of Dr. Graham Holloway. His interests involve mitochondrial bioenergetics and redox balance in the context of insulin resisitance, obesity and exercise.

Greggio et al., 2017; Hoppeler et al., 1973; Meinild Lundby et al., 2018; Nielsen et al., 2017), suggesting a complex interplay of mechanisms coordinating mitochondrial adaptations to exercise. These mitochondrial responses coincide with exercise-induced improvements in glucose homeostasis, skeletal muscle insulin signalling, cardiovascular function, cognitive capacity, and bone mineral density (Coetsee & Terblanche, 2017; Lavie et al., 2015; Luciano et al., 2002; Saltin et al., 1979; Snow-Harter et al., 1992; Zhang et al., 2023). While mitochondrial adaptations and exercise-induced health benefits appear to be exercise intensity/duration agnostic within muscle, contemporary research has challenged this notion. Excessive exercise training volumes have been implicated in multiple adverse health outcomes. This includes compromising cardiac function, inducing cardiac arrhythmias and atrial fibrillation, accelerating coronary calcification and atherosclerosis, and promoting myocardial fibrosis. Additionally, excessive training can disrupt skeletal muscle homeostasis through structural damage to fibre ultrastructure and inflammatory responses, impair glucose homeostasis, exacerbate liver fibrosis,- and potentially compromise cognitive function (Eijsvogels et al., 2018; Flockhart et al., 2021; Liu et al., 2025; Ramos-Cabrer et al., 2025; Symons et al., 2023).

Overtraining, defined as performing intensified training that may lead to underperformance indicative of overreaching (Meeusen et al., 2013), raises important questions about the limits of metabolic plasticity in highly trained individuals. While overtraining can lead to overreaching, not all individuals subjected to intensified training reach this state and may instead be classified as acutely fatigued. Indeed, when training loads become excessive, overtraining appears to induce hepatic fibrosis and activate myeloid cell leukaemia sequence 1 (MCL1)–BAX/BAK-mediated apoptotic signalling, impairing the function of the liver (Liu et al., 2025). While alterations in hepatic stress-signalling could contribute to excessive-exercise impairments in whole-body glucose homeostasis, the impact of overtraining on skeletal muscle insulin responsiveness remains debatable. Within muscle, increased mitochondrial-derived reactive oxygen species (mtROS) and the associated redox-mediated signalling events have a well-defined role in the induction of insulin resistance in overnutrition contexts (Fisher-Wellman & Neufer, 2012). Surprisingly, despite the induction of whole-body glucose intolerance, excessive exercise training reduces mtROS (Cardinale et al., 2021; Flockhart et al., 2021), a response that would be expected to increase skeletal muscle insulin signalling. The apparent paradox suggests the impairment in glucose homeostasis extends beyond skeletal muscle dysfunction (Liu et al., 2025). Therefore, the notion that excessive exercise training impairs skeletal muscle mitochondrial bioenergetics or skeletal muscle insulin signalling remains an open question.

Table 1. Characteristics of participants before the overtraining protocol

Age (years)	25.2 ± 3.0
Body mass (kg)	76.6 ± 15.2
Height (cm)	176.1 ± 12.3
BMI (kg m^{-2})	24.5 ± 2.6
Time Trial $\dot{V}_{O_2}$ (ml kg^{-1} min^{-1})	56.2 ± 8.0

Note: Data presented as means ± standard deviation. Abbreviations: BMI, body mass index; $\dot{V}_{O_2}$, oxygen consumption during time trial.

Herein, we sought to determine the mitochondrial and proteome adaptations in skeletal muscle of highly trained endurance athletes by increasing their already substantial training load. We hypothesized that overtraining endurance trained athletes would alter mtROS and affect skeletal muscle insulin signalling and mitochondrial function. We found that overtraining highly trained individuals elicited mitochondrial biogenesis and improvements in insulin signalling in skeletal muscle. Our data indicate the absence of mitochondrial dysfunction or the development of skeletal muscle insulin resistance following intensified training in this population.

Methods

Participants

Nine endurance athletes (77 males, 2 females; Table 1) volunteered to participate in the study. All participants self-reported as actively training a minimum of 7 h per week in endurance activities (running, cycling, swimming, or rowing) prior to study commencement. The study conformed to the standards set by the *Declaration of Helsinki*, except for registration in a database. Participants were excluded if they reported any cardiovascular, metabolic or musculoskeletal conditions, or were taking medications that could affect the study outcomes. This study formed part of a larger collaborative research investigation (Coates et al., 2024; Ranahan et al., 2025; Roussel et al., 2024), and was approved by the University Research Ethics Board (REB#21-11-017). All participants provided written informed consent before participation.

Study design and overtraining protocol

To establish baseline training load, participants recorded their typical training using an online activity tracking

application (Strava Inc®, San Francisco, CA, USA) for minimally 1 week prior to study commencement. A single investigator then programmed individualized training plans for the 4-week study in consultation with each participant.

The study consisted of a 4-week protocol divided into one baseline week and 3 weeks of intensified training as detailed previously (Coates et al., 2024). In brief, during the baseline week (Week 1), participants were instructed to reduce their normal training hours by approximately 50% to ensure adequate recovery. This was followed by a 3-week intensified training period (Week 2–4) where participants completed their regular training sessions outside of the laboratory in addition to three supervised high-intensity sessions per week in the laboratory, targeting an overall training duration of approximately 150% of their pre-study levels.

The supervised visits, as detailed previously (Coates et al., 2024), included two Wingate-based sprint interval training sessions and one 5-km time trial (TT) per week. The Wingate-based sprint interval training sessions consisted of repeated 30-s maximal sprints on a cycle ergometer (Velotron, Racermate, Seattle, WA, USA) against a resistance of 7.5% body mass, with 4 min of active recovery (cycling at 50 W) between sprints. The number of sprints progressed weekly: Week 2: 4 × 30 s; Week 3: 5 × 30 s; Week 4: 6 × 30 s. The 5-km TT was performed on the same cycle ergometer, with participants instructed to complete the distance as quickly as possible. During the 5-km TT visit in Week 1 and 4, participants completed the Hooper–Mackinnon well-being questionnaire (Hooper & Mackinnon, 1995), from which a composite mood score was calculated. Expired gases were collected breath-by-breath during the TT using open-circuit indirect calorimetry to determine oxygen consumption ($\dot{V}_{O_2}$). Capillary blood lactate concentration was determined via fingertip puncture (Lactate Plus, Nova Biomedical, Waltham, MA, USA) prior to the start and within 1 min of 5-km-TT completion to determine resting and lactate TT peak. All laboratory sessions were separated by approximately 48 h. Participants recorded their additional training sessions using a mobile application (Strava, Inc.).

Oral glucose tolerance test. Following an overnight fast, participants consumed 75 g of glucose (Trutol, Thermo Fisher Scientific, Waltham, MA, USA) and remained seated for 2 h. Blood glucose concentrations were assessed via finger capillary sampling at 0, 15, 30, 45, 60, 90 and 120 min and determined immediately via a handheld glucometer (Verio Reflect, OneTouch, Zug, Switzerland). Additional capillary blood samples for serum insulin were collected at baseline and at 30 min following the ingestion of glucose and spun at 1200 *g* for 15 min for insulin concentration analysis. Insulin concentration was assessed in duplicate using an ELISA kit (cat. no. KAQ1251, Thermo Fisher Scientific, Mississauga, ON, Canada). The area under the curve for blood glucose was calculated using the trapezoidal rule to assess glucose tolerance.

Muscle biopsies. Muscle samples were obtained from the vastus lateralis before the overtraining period (Pre) and approximately 72 h after the last 5-km time trial and/or intense training session (Post) with no more than 1 h of low intensity exercise the day prior to each biopsy. Participants were instructed to abstain from caffeine, stimulants, recreational drugs and alcohol for 24 h, and food/liquid for 12 h before each biopsy visit. During each sampling visit, a biopsy was obtained in basal condition where an aliquot was immediately placed in ice-cold BIOPS (2.77 mM CaK_2EGTA, 7.23 mM K_2EGTA, 5.77 mM Na_2ATP, 6.5 mM $MgCl_2{}^*6H_2O$, 15 mM Na_2PCr, 20 mM imidazole, 0.5 mM dithiothreitol and 50 mM MES) for preparation of permeabilized muscle fibres while the remaining sample was flash frozen in liquid nitrogen for western blotting and proteomic analysis. A secondary biopsy was obtained 30 min after the consumption of 75 g glucose (post-glucose; Trutol) and flash frozen in liquid nitrogen for subsequent western blotting. All biopsies were performed under local anaesthesia (2% lidocaine with adrenaline) utilizing a Bergstrom needle.

Protein extraction and purification for liquid chromatography–mass spectrometry

Protein extraction and bottom-up unlabelled proteomics were performed as previously described (Frangos et al., 2025). Briefly, 25 µg of protein per lysate was resolubilized in denaturation buffer (6 M urea/2 M thiourea) and simultaneously reduced with 10 mM DTT and alkylated with 20 mM iodoacetamide at room temperature for 60 min. Samples were precipitated by adding 6:1 v/v cold acetone and kept at −80°C for 60 min. The resulting pellet was collected after centrifugation at 10,000 *g* for 10 min at 4°C and resuspended with 50 mM ammonium bicarbonate and MD-grade trypsin (Thermo Fisher Scientific, cat. no. 90057) 1:50 protease to protein ratio for overnight digestion at 37°C. Following digestion, samples were vacuum dried and purified using Pierce C18 Spin columns (Thermo Fisher Scientific, cat. no. 89873).

The Vanquish Neo UHPLC system was coupled with Orbitrap Exploris 240 mass-spectrometer equipped with an Easy-Spray source for nanoLC-MS protein identification. Mobile phase A and weak wash liquid consisted of water with 0.1% formic acid, while mobile phase B and strong wash liquid contained 80% acetonitrile with 0.1% formic acid. The Orbitrap Exploris 240 MS was operated in data-dependent acquisition mode, acquiring

full scan MS1 spectra acquired over an m/z range 375–1500.

Proteomics data analysis

Analysis of the tissue proteome was performed in R (version 4.2.1) and R Studio (version 2024.04.2+764). Principal component analysis was performed using the Vegan package. Volcano plots were created using $\log_2$transformed fold change and $-\log_{10}$ adjusted P-value. P-values of differentially regulated proteins between groups were corrected as adjusted P-values by applying false discovery rate available in the Deseq2 package. Depending on the analysis, heatmaps and volcano plots were generated using all detected proteins or proteins sorted by P_{adjust} <0.1, gene ontology or MitoCarta3.0, detailed descriptions for each analysis are included in the figure descriptions. Gene set enrichment was performed with the Kyoto Encyclopedia of Genes and Genomes (KEGG; Kanehisa et al., 2016) and EnrichR (Xie et al., 2021).

Permeabilized muscle fibres

Permeabilized muscle fibre bundles were separated under a microscope in ice cold BIOPS utilizing fine-tipped forceps, treated with 40 mg mL^{-1} saponin for 30 min at 4°C, and then washed in mitochondrial respiration medium (MiR05; 0.05mM EGTA, 3mM $MgCl_2{}^*H_2O$, 60 mM potassium lactobionate, 10 mM KH_2PO_4, 20 mM HEPES, 110 mM sucrose and fatty acid-free BSA (1 g L^{-1})) for mitochondrial respiration or Buffer Z (105 mM K-MES, 30 mM KCl, 1 mM EGTA, 10 mM K_2HPO_4, 5 mM $MgCl_2.H_2O$, 0.005 mM pyruvate, 0.002 mM malate and fatty acid-free BSA (5 mg mL^{-1})) for H_2O_2 emission measurements as previously published (Miotto et al., 2018; Smith et al., 2013).

High-resolution respirometry

Mitochondrial respiration experiments were performed in a high-resolution respirometer (Oroboros O2k, Innsbruck, Austria) at 37°C with constant stirring (750 rpm) in the presence of 5 μM blebbistatin. ADP titration (25, 100, 175, 250, 500, 1000, 2000, 4000, 6000, 8000, 10,000 μM with additional 2000 μM addition until a plateau is reached) was performed in the presence of 5 mM pyruvate and 1 mM malate followed by a sequential addition of 10 mM glutamate, 10 mM succinate and 10 μM cytochrome *c*. The wet weight of fibres was obtained prior to starting the respiration experiment and the protocol was performed in duplicate with the average per participant reported. Mitochondrial respiration rates were normalized to individual fibre wet weight and the participant's skeletal muscle mitochondrial content estimated by calculated mitochondrial enrichment factor (MEF) based on all detected mitochondrial proteins by quantitative label-free proteomics (Human MitoCarta 3.0 database; Rath et al., 2021) normalized to individual fibre weight similarly to previously described (McLaughlin et al., 2020).

H_2O_2 emission

Mitochondrial H_2O_2 emission in permeabilized fibres was determined fluorometrically (Lumina, Thermo Fisher Scientific) in a constantly stirring cuvette at 37°C containing a standard reaction buffer (Buffer Z) supplemented with 20 μM blebbistatin, 40 U mL^{-1} CuZnSOD, 10 μM Amplex Red (Thermo Fisher Scientific) and 0.5 U mL^{-1} horseradish peroxidase as previously described. Mitochondrial H_2O_2 emission rates were determined with the addition of 20 mM succinate to promote H_2O_2 production followed by the addition of 100 μM ADP to attenuate H_2O_2 production. All samples were run in duplicate with the average reported and normalized to individual fibre wet weight and the participant's mitochondrial content similarly to mitochondrial respiration. A standard curve for all experiments was made with a known concentration of H_2O_2.

Western blotting

Skeletal muscle biopsies were homogenized in lysis buffer, diluted to 1 μg μL^{-1} and loaded equally onto standard SDS-PAGE gel, transferred to polyvinylidene difluoride membranes and incubated in the appropriate blocking solution according to the antibody as previously reported (Holloway et al., 2018). Primary antibody targets include: total-Akt (1:1000, Cell Signaling Technology, Danvers, MA, USA, cat. no. 4691), phosphorylated Akt-Ser473 (1:1000, Cell Signaling Technology cat. no. 9271), Akt-Thr308 (1:1000, Cell Signaling Technology cat. no. 9275), nitrotyrosine (1:500, Cayman Chemical Co., Ann Arbor, MI, USA, cat. no. 189542), *trans*-4-hydroxy-2-nonenal (4HNE; 1:1000, Alpha Diagnostics, cat. no. HNE-11s, San Antonio, TX, USA). All membranes were imaged using enhanced chemiluminescence (ChemiGenius2 Bioimaging System, SynGene, Cambridge, UK), quantified with the FluorChem HD imaging chemiluminescence (Alpha Innotech, San Leandro, CA, USA). α-Tubulin was used as a loading control.

Participant categorization criteria

In accordance with the terminology highlighted by Meeusen and colleagues (2013), overtraining was defined

Table 2. Whole-body adaptation to the overtraining protocol

	Pre-overtraining	Post-overtraining	*P*
Body mass (kg)	76.6 ± 15.2	76.7 ± 14.8	0.993
BMI (kg m$-^2$)	24.5 ± 2.6	24.5 ± 2.5	0.968
Time trial (s)	477 ± 59	481 ± 62	0.041
Time trial $\dot{V}_{O_2}$ (ml kg^{-1} min^{-1})	56.2 ± 8.0	52.7 ± 7.15	0.042
Mood score	22.2 ± 3.7	30.7 ± 4.4	<0.001
Resting lactate (mmol L^{-1})	1.47 ± 0.4	1.02 ± 0.4	0.014
Lactate TT peak (mmol L^{-1})	13.6 ± 2.7	10.4 ± 2.72	0.001

Note: Data presented as means ± standard deviation for each group. Statistical test: paired two-tailed Student's *t* test. Mood score, sum score of fatigue, stress, sleep, muscle soreness, training enjoyment and irritability; resting lactate, lactate measured at the start of the time trial test; lactate TT peak, lactate measured at the end of the time trial test; time trial $\dot{V}_{O_2}$, oxygen consumption during TT. Abbreviations: BMI, body mass index; TT, time trial.

as the process of intensified training resulting in two distinct outcomes: overreaching or acute fatigue. Overreached participants were defined as those demonstrating negative psychophysiological adaptations following the overtraining protocol, whereas acutely fatigued participants did not. Specifically, we utilized three psychophysiological parameters to define overreaching: (i) reduced time trial performance post-training, (ii) mood alteration scores exceeding 4 (on a 5-point scale), and (iii) decreased force production during low-frequency electrical stimulation (Coates et al., 2024; Roussel et al., 2024). Using these criteria, six participants were classified as overreached and three as acutely fatigued.

Statistical analysis

All data were analysed using GraphPad Prism 10.0 (GraphPad Software, Boston, MA, USA), except for proteomic analyses which were performed using R Studio (version 2024.12.1+563). The Shapiro–Wilk test was used to assess normality of data distribution. For comparisons between pre- and post-overtraining time points, normally distributed data were analysed using a paired two-tailed Student's *t* test, while non-normally distributed data were analysed using Wilcoxon's matched-pairs signed rank test. Changes in glucose tolerance across pre- and post-overtraining time points were evaluated using two-way repeated measures ANOVA followed by Tukey's *post hoc* test where appropriate. Statistical comparisons between overreached and acutely fatigued groups were performed using a two-tailed unpaired Student's *t* test for normally distributed data, while the Mann–Whitney *U*-test was applied when data did not pass the Shapiro–Wilk normality test. For mitochondrial function and western blot analyses, statistical significance was set at $P < 0.05$. For proteomic analyses, differences were considered statistically significant at an adjusted *P*-value <0.1 obtained by applying a false discovery rate (FDR) correction. All codes used in this study are publicly available at: https://github.com/henver-brunetta/Muscle-overtraining.

Results

Overtraining upregulates protein expression related to energy metabolism

Nine participants successfully completed the 4-week exercise protocol (baseline week at approximately 70% volume pre-study + 3 weeks overtraining at 150% volume pre-study levels; Fig. 1*A*). As expected, the overtraining protocol increased the time to cycle 5 km, as well as reduced $\dot{V}_{O_2}$ and peak lactate during the time trial test (Table 2). Additionally, the overtraining protocol increased mood score, indicating more fatigue, irritability and stress in the participants (Table 2). Importantly, overtraining protocol did not affect body weight nor BMI, indicating that even though the participants underwent an overall increase in fatigue, energy balance appeared to be maintained.

Having characterized the physiological responses to overtraining, we next sought to characterize the skeletal muscle adaptations associated with the 3 weeks of overtraining in these endurance athletes (Fig. 1*A*). Specifically, we assessed protein levels pre- and post-overtraining by applying bottom-up quantitative label-free proteomics in vastus lateralis biopsies obtained at baseline and following the completion of the overtraining protocol. Our analysis identified 1442 proteins in both the pre- and post-overtraining samples in all participants (Supporting information, Table S1), with 805 showing differential expression (Fig. 1*B*, adjusted *P*-value <0.1). The volcano plot shows a clear pattern of protein upregulation across the data set following exercise training compared to baseline levels (Fig. 1*C*). To better understand the biological implications of these changes, we performed an enrichment analysis with the differentially

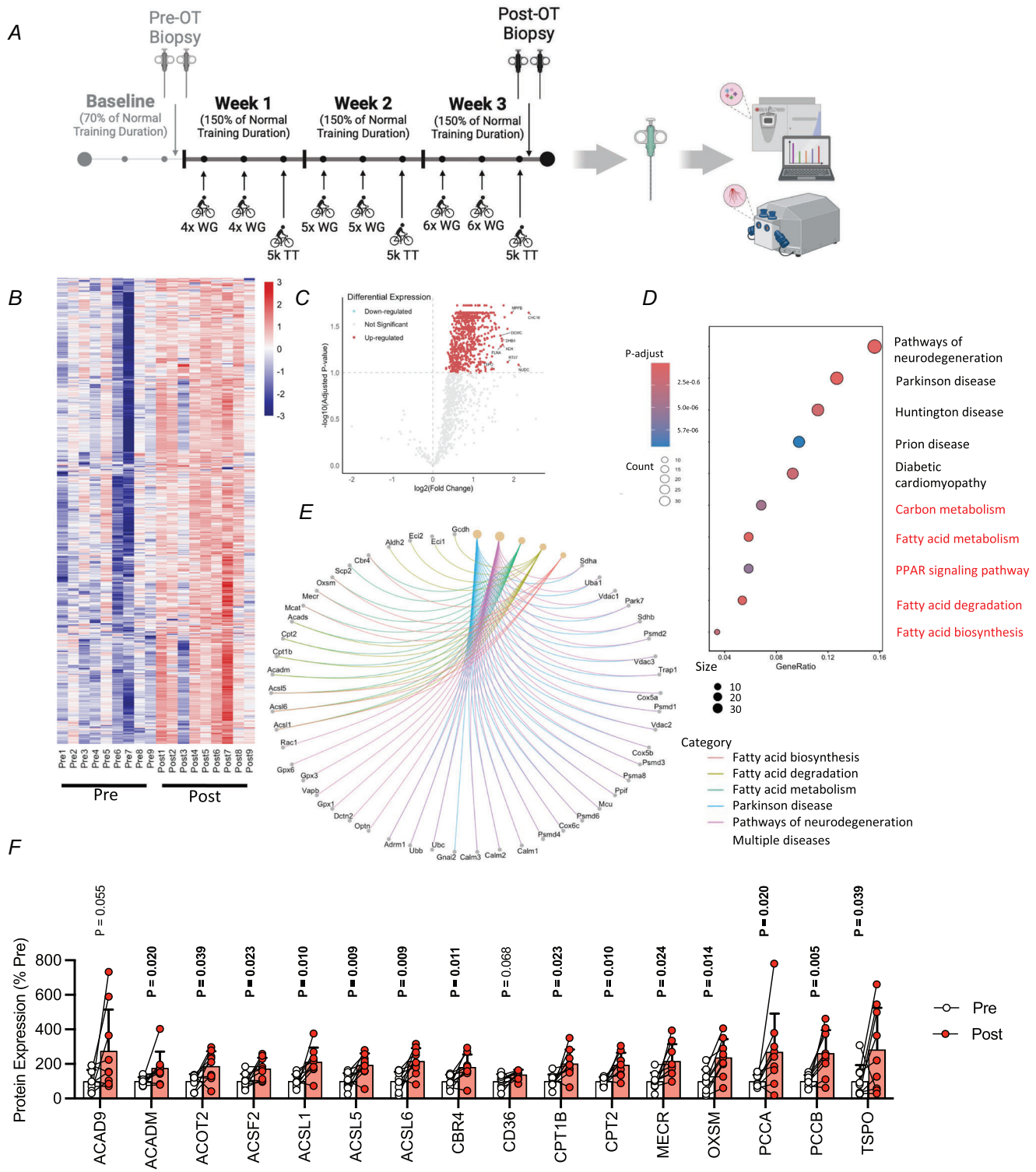

Figure 1. Overtraining increases protein content
A, schematic representation of the study design (n = 9/condition). *B*, heatmap of 805 proteins differentially expressed (adjusted *P*-value of <0.1). *C*, volcano plot showing all identified proteins between pre-overreaching and post-overreaching. *D*, KEGG enrichment analysis of 805 differentially expressed proteins. *E*, associated gene-concept network of top 5 pathways. *F*, lipid-related metabolic proteins. B, For the proteomic analysis an adjusted *P*-value of <0.1 was considered statistically significant. F, Data expressed as means ± SD and

were assessed for normality using the Shapiro-Wilk test. Data which met the assumption of normality were analysed using a paired two-tailed Student's *t*-test, while the remaining data that did not pass the normality test were analysed using Mann–Whitney test (*i.e.,* ACAD9, ACADM, ACOT2, TSPO). Bolded *P*-values are indicated for comparisons with a *P*-value of < 0.05. Each individual point represents a biological sample. ACAD9, acyl-CoA dehydrogenase family member 9; ACADM, acyl-CoA dehydrogenase medium chain; ACOT2, acyl-coenzyme A thioesterase 2; ACSF2, acyl-CoA synthetase family member 2; ACSL1, acyl-CoA synthetase long chain family member 1; ACSL5, acyl-CoA synthetase long chain family member 5; ACSL6, acyl-CoA synthetase long chain family member 6; CBR4, 3-oxoacyl-[acyl-carrier-protein] reductase; CD36, cluster of differentiation 36; CPT1B, carnitine palmitoyltransferase 1b; CPT2, carnitine palmitoyltransferase 2; $\log_2$FC, log2 fold change; MECR, mitochondrial *trans*-2-enoyl-CoA reductase; OXSM, 3-oxoacyl-[acyl-carrier-protein] synthase, mitochondrial; PCCA, propionyl-CoA carboxylase alpha chain; PCCB, propionyl-CoA carboxylase beta chain; TSPO, translocator protein; TT, time trial; WG, Wingate test.

expressed proteins (Fig. 1*D*, adjusted *P*-value <0.1). KEGG analysis revealed enrichment in several key pathways involved in canonical exercise adaptations, including carbon metabolism, lipid biosynthesis and degradation, and peroxisome proliferator-activated receptor (PPAR) signalling, a classical modulator of mitochondrial biogenesis (Perry et al., 2010). These pathways were further confirmed by a concept network diagram (Fig. 1*E*) showing lipid metabolism being one of the primary affected pathways in the overtrained muscle samples with numerous differentially expressed proteins, including an increase in ACAD9 ($P = 0.055$), ACADM ($P = 0.020$), ACOT2 ($P = 0.039$), ACSP2 ($P = 0.023$), ACSL1 ($P = 0.010$), ACSL5 ($P = 0.009$), ACSL6 ($P = 0.009$), CBR4 ($P = 0.011$), CD36 ($P = 0.068$), CPT1B ($P = 0.023$), CPT2 ($P = 0.010$), MECR ($P = 0.024$), OXSM ($P = 0.014$), PCCA ($P = 0.020$), PCCB ($P = 0.005$) and TSPO ($P = 0.039$) (Fig. 1*F*; definitions of abbreviations in Fig. 1 legend). Together, these findings demonstrate the capacity of trained athletes to upregulate proteins involved in metabolism and mitochondrial biogenesis in response to overload training.

Overtraining enhances mitochondrial function, despite increased oxidative stress

Given the substantial upregulation in energy metabolism-related proteins following 3 weeks of overtraining, we next investigated whether these changes translated to functional adaptations in mitochondrial bioenergetics. Specifically, in saponin-permeabilized muscle fibres, we found that both maximal complex-I, maximal complex-I/II-linked oxidative phosphorylation (Fig. 2*A*; +ADP (+D), $P = 0.031$; +glutamate (+G), $P = 0.046$; and +succinate (+S), $P = 0.055$) and respiratory control ratio (Fig. 2*B*, $P = 0.045$) were higher in athletes after completing the overtraining programme. Given acute and chronic exercise modulate mitochondrial ADP sensitivity (Ludzki et al., 2015; Miotto & Holloway, 2019; Petrick & Holloway, 2019), we next performed an ADP titration in energized mitochondria to determine mitochondrial ADP sensitivity following overtraining. The concentration of ADP required to reach 50% of maximal ADP-supported respiration showed an increased trend in the after overtraining (Fig. 2*C* and *D*, $P = 0.098$), possibly linked to the increased respiration in the presence of near maximal ADP concentrations (Fig. 2*E*; $P > 0.999$, 25 μM; $P = 0.570$, 100 μM; $P = 0.734$, 175 μM; $P = 0.550$, 250 μM; $P = 0.753$, 500 μM; $P = 0.764$, 1000 μM; $P = 0.622$, 2000 μM; $P = 0.1023$, 4000 μM; $P = 0.0360$, 6000 μM; $P = 0.0131$, 8000 μM; $P = 0.0149$, 10,000 μM). Since our initial respiratory measurements were normalized to wet fibre weight, which can be influenced by mitochondrial content within skeletal muscle, we next calculated the MEF in our bulk proteome by filtering out mitochondrial proteins listed in MitoCarta3.0 to determine if the increased maximal respiration was driven by the induction of mitochondrial biogenesis. Of the 1441 conserved proteins detected, 152 were identified within the mitochondrial proteome. The volcano plot revealed that the majority of the mitochondrial proteome (i.e., 113 proteins) was upregulated following overtraining (Fig. 2*G*), which cumulated to an increased MEF (Fig. 2*H*, $P = 0.018$). Highlighting the effects of exercise in mitochondrial respiratory capacity and substrate oxidation, most of the upregulated proteins were found in 'metabolism', 'lipid metabolism', 'OXPHOS', 'fatty acid oxidation' and 'carbohydrate metabolism' MitoCarta3.0 pathways (Fig. 2*I*). This canonical adaptation induced by exercise within skeletal muscle was positively correlated with maximal complex-I/II-linked respiration (Fig. 2*J*, $r = 0.6793$, $P = 0.002$). Notably, when normalized to MEF, mitochondrial respiration was not different following overtraining in the presence of any of submaximal (data not shown) or maximal ADP concentrations or maximal complex-I nor maximal complex-I/II-linked oxidative phosphorylation (Fig. 2*K*, $P = 0.570$ +D, $P = 0.359$ +G, $P = 0.359$ +S). The data suggest the training-induced increase in maximal ADP-supported respiration was driven primarily by the induction of mitochondrial biogenesis, and unlike previous reports (Flockhart et al., 2021), suggests the absence of an intrinsic mitochondrial respiratory dysfunction following an overtraining protocol.

While excessive training has been reported to lower the intrinsic mitochondrial capacity for H_2O_2 emission, increased mitochondrial enzymatic abundance is associated with greater capacity for mtROS production (Neurohr et al., 2021). We next examined mitochondrial H_2O_2 emission in permeabilized fibres. Succinate-driven mitochondrial H_2O_2 emission was increased following overtraining both in the presence and absence of ADP (Fig. 3*A* and *B*, $P = 0.039$ and $P = 0.027$). Additionally, in support of a trend for reduced ADP respiratory sensitivity, the ability of ADP to suppress H_2O_2 emission was attenuated in skeletal muscle fibres post-training (Fig. 3*B* inset, $P = 0.019$). Although 4HNE levels did not change (Fig. 3*C* and *D*, $P = 0.730$), the increased capacity for mitochondrial H_2O_2 emission coincided with elevated nitrotyrosine protein levels (Fig. 3*C* and *D*, $P = 0.026$), a marker of NO-dependent protein modification, despite increased expression of several mitochondrial antioxidant defence proteins, including superoxide dismutase 1 (SOD1; $P = 0.023$), catalase (CAT; $P = 0.030$), glutathione peroxidase 1/4 (GPX1/4; $P = 0.026/P = 0.048$), peroxiredoxin 6 (PRDX6;

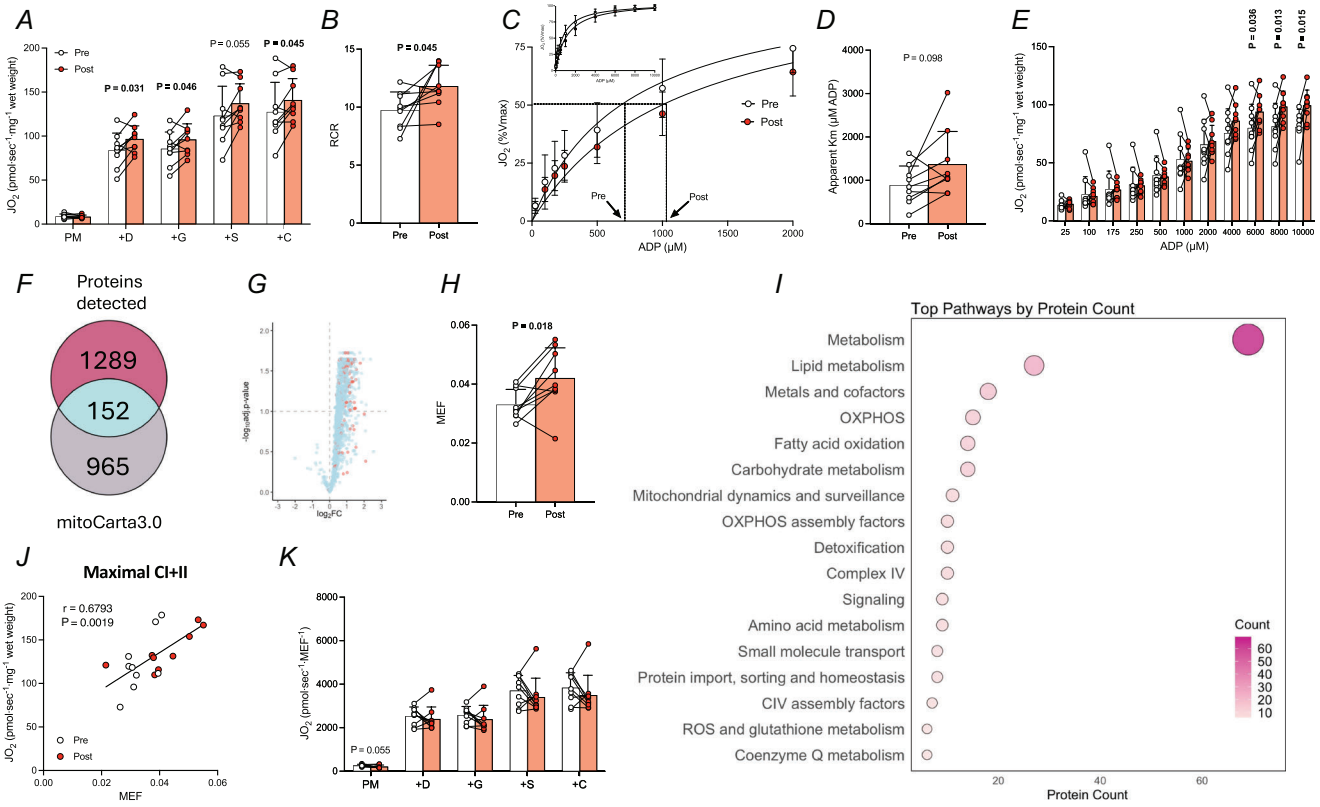

Figure 2. Mitochondrial bioenergetics assessment in response to overtraining
A, mitochondrial respiration in the presence of various saturating complex I- and II-linked substrates normalized to fibre wet weight ($n = 9$/condition). The +D state represents the maximal ADP-supported respiration value obtained during the ADP titration phase. *B*, respiratory control ratio. *C*, mitochondrial kinetics for ADP-supported respiration from the ADP titration phase. *D*, apparent ADP K_m. *E*, associated absolute values. *F*, Venn diagram of total proteins detected and mitochondrial proteins in accordance with the Human.MitoCarta3.0. *G*, volcano plot showing all identified proteins between pre-overreaching and post-overreaching, highlighting mitochondrial proteins (red) and non-mitochondrial proteins (blue). *H*, mitochondrial enrichment fraction (MEF). *I*, top pathways enriched among upregulated mitochondrial proteins. *J*, correlation analysis of maximal complex I (CI) and complex II (CII) linked respiration with MEF. *K*, mitochondrial respiration in the presence of various saturating CI and CII-linked substrates normalized to MEF. Data expressed as means ± SD. Mitochondrial function and MEF measurements were assessed for normality using the Shapiro–Wilk test. Data that passed the Shapiro–Wilk test were analysed using a paired two-tailed Student's *t* test, while data that did not pass the normality test were analysed using Wilcoxon test (*D*, *E*, 25 μM, *K*, 100 μM). Bolded *P*-values are indicated for comparisons with a *P*-value of <0.05. Each individual point represents a biological sample. ADP, adenosine diphosphate; +C, +cytochrome *c*; +D, +ADP; +G, +glutamate; JO_2, oxygen consumption rate; MEF, mitochondrial enrichment factor; PM, pyruvate + malate; RCR, respiratory control ratio; +S, +succinate; V_{max}, maximal velocity.

$P = 0.034$) (Fig. 3*E*, bolded adjusted *P*-value <0.1). Similar to mitochondrial respiratory capacity, we observed a positive correlation between mtROS production and mitochondrial content in both state 3 and state 4 that were tested (Fig. 3*F* and *G*, $r = 0.7529$, $P = 0.0003$ and $r = 0.7076$, $P = 0.001$, respectively). Indeed, normalization of mtROS emission by mitochondrial content abrogated the effects of overtraining in the presence of succinate but not in the presence of ADP (Fig. 3*H*, $P = 0.143$ and $P = 0.040$). The persistence of redox imbalance despite increased antioxidant defence following overtraining raised concerns about potential metabolic consequences, particularly regarding insulin sensitivity in skeletal muscle.

Overtraining enhances insulin signalling within skeletal muscle

Given our observations of redox imbalance and the well-established link between oxidative stress and insulin resistance in skeletal muscle (Hurrle & Hsu, 2017; Rains & Jain, 2011), we next investigated whether overtraining affected insulin signalling pathways. We first filtered our proteome dataset against the KEGG insulin signalling pathway (hsa04910). A heatmap visualization (Fig. 4*A*) revealed widespread upregulation of proteins (bolded adjusted *P*-value <0.1) within the interconnected insulin signalling network, including those involved in glucose uptake and metabolic pathways (i.e., SLC2A4/GLUT4,

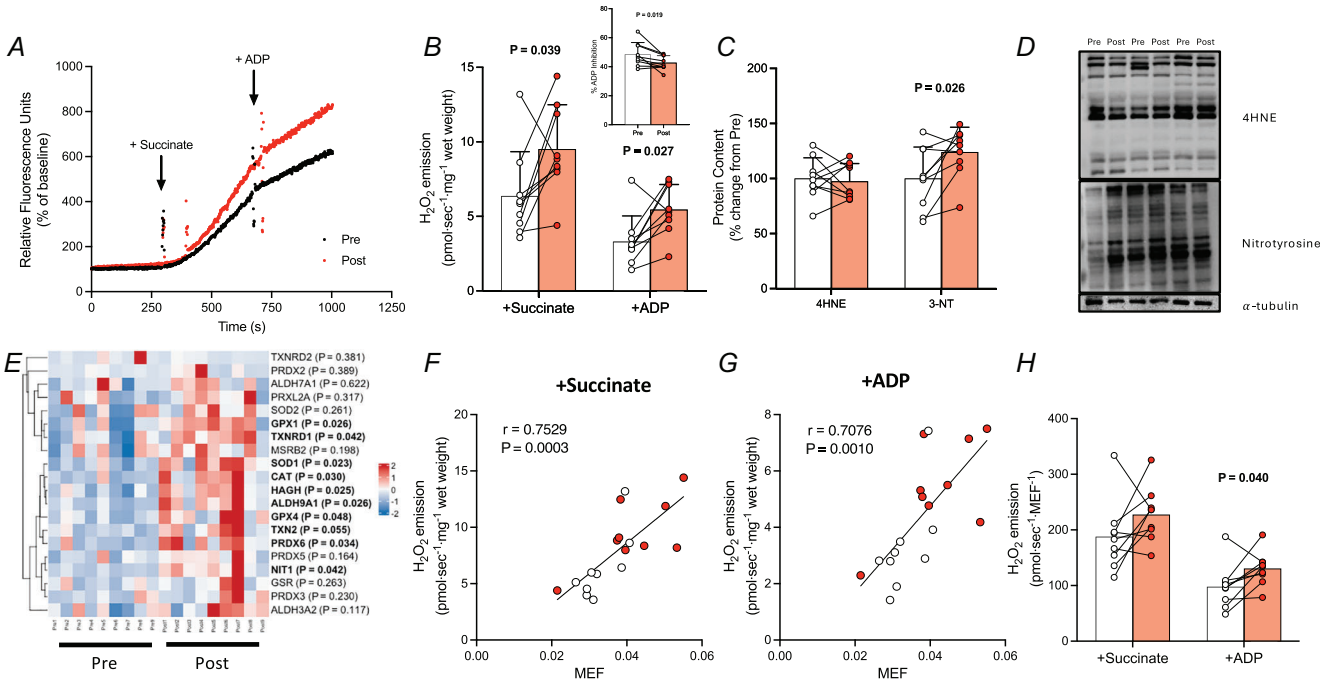

Figure 3. Mitochondrial redox balance following an overtraining protocol
A and *B*, representative traces (*A*) and measurements of mitochondrial H_2O_2 emission (*B*) in the presence of succinate and attenuation with the addition of ADP. Inset shows the percentage of ADP inhibition normalized to fibre wet weight (n = 9/condition). *C*, protein content of 4HNE-modified protein and 3-NT quantified as a percentage of pre-overreaching. *D*, representative western blot. *E*, heatmap of identified proteins related to ROS and glutathione metabolism from MitoPathway3.0 database; the *P*-value was bolded if the adjusted *P*-value was < 0.1. *F* and *G*, correlation analyses of mitochondrial H_2O_2 emission in the presence of succinate (*F*) and ADP (*G*) with MEF. *H*, measurements of mitochondrial H_2O_2 emission in the presence of succinate and attenuation with the addition of ADP normalized to MEF. Data expressed as means ± SD. Mitochondrial H_2O_2 emission and measurements were assessed for normality using the Shapiro–Wilk test. Data that passed the Shapiro–Wilk test were analysed using a paired, two-tailed Student's *t*-test, while data that did not pass the normality test were analysed using Wilcoxon test (*B*, +succinate, +ADP). Bolded *P*-values are indicated for comparisons with a *P*-value of <0.05. Each individual point represents a biological sample. ADP, adenosine diphosphate; ALDH3A2, aldehyde dehydrogenase 3 family member a2; ALDH7A1, aldehyde dehydrogenase 7 family member a1; ALDH9A1, aldehyde dehydrogenase 9 family member a1; CAT, catalase; GPX1, glutathione peroxidase 1; GPX4, glutathione peroxidase 4; GSR, glutathione reductase; H_2O_2, hydrogen peroxide; HAGH, hydroxyacylglutathione hydrolase; 4-HNE, 4-hydroxynonenal; MSRB2, methionine sulfoxide reductase b2; NIT1, nitrilase 1; 3-NT, nitrotyrosine; PRDX2, peroxiredoxin 2; PRDX3, peroxiredoxin 3; PRDX5, peroxiredoxin 5; PRDX6, peroxiredoxin 6; PRXL2A, peroxiredoxin like 2a; ROS, reactive oxygen species; SOD1/2, superoxide dismutase 1/2; TXN2, thioredoxin 2; TXNRD1/2, thioredoxin reductase 1/2

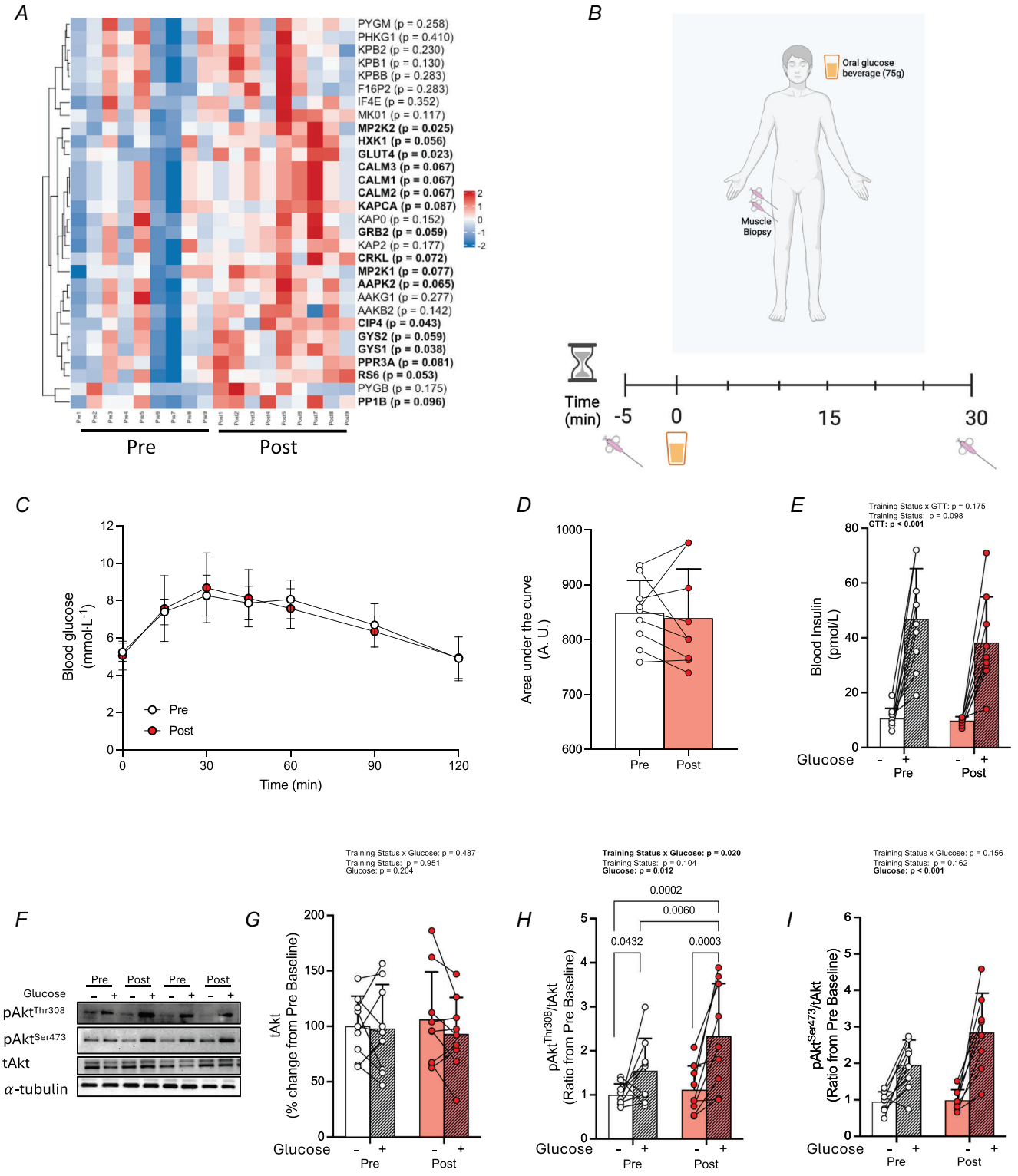

Figure 4. Overtraining improves insulin signalling and glucose metabolism
A, heatmap of identified proteins involved in insulin signalling pathways (KEGG pathway hsa04910 database); *P*-value was bolded if the adjusted *P*-value was <0.1. *B*, schematic representation of glucose tolerance protocol. *C–E*, blood glucose (*C*), respective area under the curve (*D*) and blood insulin concentration (*E*) during an oral glucose tolerance test. *F*, representative image of a western blot used to quantify protein content. *G–I*, tAKT (*G*), pAkt^{Thr308}:tAkt (*H*) and pAkt^{Ser473}:tAkt (*I*). Blood glucose area under the curve was assessed for normality using

the Shapiro–Wilk test and was analysed using a paired, two-tailed Student's *t*-test. Blood insulin and western blot were compared by a two-way repeated measure ANOVA. Bolded *P*-values are indicated for comparisons with a *P*-value of <0.05 with an *n* = 8–9/condition. Each individual point represents a biological sample. AAKB2, protein kinase amp-activated non-catalytic subunit beta 2; AAKG1, protein kinase amp-activated non-catalytic subunit gamma 1; AAPK2, 5′-AMP-activated protein kinase catalytic subunit alpha-2; AKT, protein kinase B; CALM1/2/3, calmodulin 1/2/3; CIP4, CDC42-interacting protein 4; CRKL, CRK like proto-oncogene; IF4E, eukaryotic translation initiation factor 4e; F16P2, fructose-1,6-bisphosphatase 2; GLUT4, glucose transporter type 4; GRB2, growth factor receptor bound protein 2; GYS1/2, glycogen synthase 1/2; HXK1, hexokinase 1; KAP0, cAMP-dependent protein kinase type I regulatory subunit; KAP2, cAMP-dependent protein kinase type II-alpha regulatory subunit; KAPCA, cAMP-dependent protein kinase catalytic subunit alpha; KPB1/2, phosphorylase B kinase regulatory subunit alpha 1/2; KPBB, phosphorylase kinase regulatory subunit beta; MK01, mitogen-activated protein kinase 1; MP2K1/2, dual specificity mitogen-activated protein kinase kinase 1/2; pAKT, phosphorylated AKT; $pAKT^{Ser473}$, AKT phosphorylated at serine 473; $pAKT^{Thr308}$, AKT phosphorylated at threonine 308; PHKG1, phosphorylase kinase catalytic subunit gamma 1; PP1B, serine/threonine-protein phosphatase PP1-beta catalytic subunit; PPR3A, protein phosphatase 1 regulatory subunit 3a; PYGB, glycogen phosphorylase, brain form; PYGM, glycogen phosphorylase, muscle form; RS6, 40s ribosomal protein s6; tAKT, total AKT.

$P = 0.023$; GYS1/2, $P = 0.038/P = 0.059$; and HXK1, $P = 0.056$), signal transduction (i.e., MP2K1/2, $P = 0.077/P = 0.025$; GRB2, $P = 0.059$; and CRKL, $P = 0.072$) and cellular response coordination (i.e., CIP4, $P = 0.043$; PP1B, $P = 0.096$; AAPK2, $P = 0.065$; and KAPCA, $P = 0.087$) (definitions of abbreviations are given in Fig. 4 legend). To validate these proteomic findings at a functional level, we performed an oral glucose tolerance test (OGTT) and measured Akt phosphorylation in skeletal muscle following an oral 75 g glucose challenge. For this assessment, we obtained blood samples over a 2-h period, and muscle biopsies were collected at two time points during each testing session: at baseline (fasting state) and 30 min following glucose ingestion. These paired biopsies were obtained pre and post the overtraining programme to examine skeletal muscle insulin signalling (Fig. 4*B*). The OGTT revealed no differences in blood glucose over time, area under the curve (Fig. 4*C* and *D* $P = 0.685$), or blood insulin following excessive training (Fig. 4*E*; Overtraining, $P = 0.098$; GTT, $P = 0.0002$; Overtraining × GTT, $P = 0.175$). Analysis of these tissue samples revealed that while total Akt content remained unchanged (Fig. 4*G*; Overtraining, $P = 0.951$; GTT, $P = 0.204$; Overtraining × GTT, $P = 0.487$), glucose ingestion increased phosphorylation levels in both Akt residues in both pre- and post-overtraining (Fig. 4*H* and *I*, main effect of glucose $P = 0.012$ and $P < 0.0001$, respectively). It has been suggested that high levels of exercise could impair insulin action in the skeletal muscle (Flockhart et al., 2021). Interestingly, however, the increase obtained by glucose ingestion after the overtraining protocol was greater than the one observed before our experimental training protocol (Fig. 4*H*, Training status × Glucose, $P = 0.020$; Pre-overtraining glucose *vs*. Post-overtraining glucose, $P = 0.006$). Collectively, these results demonstrate that 3 weeks of overtraining in endurance athletes enhances insulin signalling in skeletal muscle, highlighting the adaptive capacity of trained muscles to maintain metabolic health even under high stress conditions.

Overtraining may elicit a unique molecular fingerprint in skeletal muscle

Individual biological responses are believed to account for different physiological adaptations to exercise, including the capacity of some athletes to train at high intensity/volume without developing an overreaching phenotype. Although this theory has been largely accepted, it has been, so far, difficult to determine specific differences between individuals who positively and negatively adapt to exercise, mainly in highly trained individuals submitted to an overloading programme. In our cohort, although all individuals completed the overtraining programme ($n = 9$) and showed an overall increase in mitochondrial proteome, we noticed subtle differences that could reveal an underlying molecular signature of overreaching susceptibility. We identified overreaching status based on three psychophysiological parameters: (i) reduced time trial performance post-training, (ii) mood alteration scores exceeding 4 (on a 5-point scale), and (iii) decreased force production during low-frequency electrical stimulation (Coates et al., 2024; Roussel et al., 2024). Based on these criteria, six athletes were classified as overreached while the remaining three were categorized as acutely fatigued (Fig. 5*A*).

To investigate potential molecular signature between these distinct response groups, we reanalysed our bulk proteomic dataset (Supporting information, Table S2), focusing on exercise-induced positive variance in protein expression (average fold change >1) for each individual and compared the six individuals who were overreached to the three individuals who were not. Principal component analysis revealed a distinct separation between overreached and acutely fatigued athletes, suggesting a molecular signature associated with our psychophysiological classification method (Fig. 5*B*). Direct comparison between groups showed an overall reduction in protein levels in the overreached athletes (Fig. 5*C*), despite these proteins being overall up

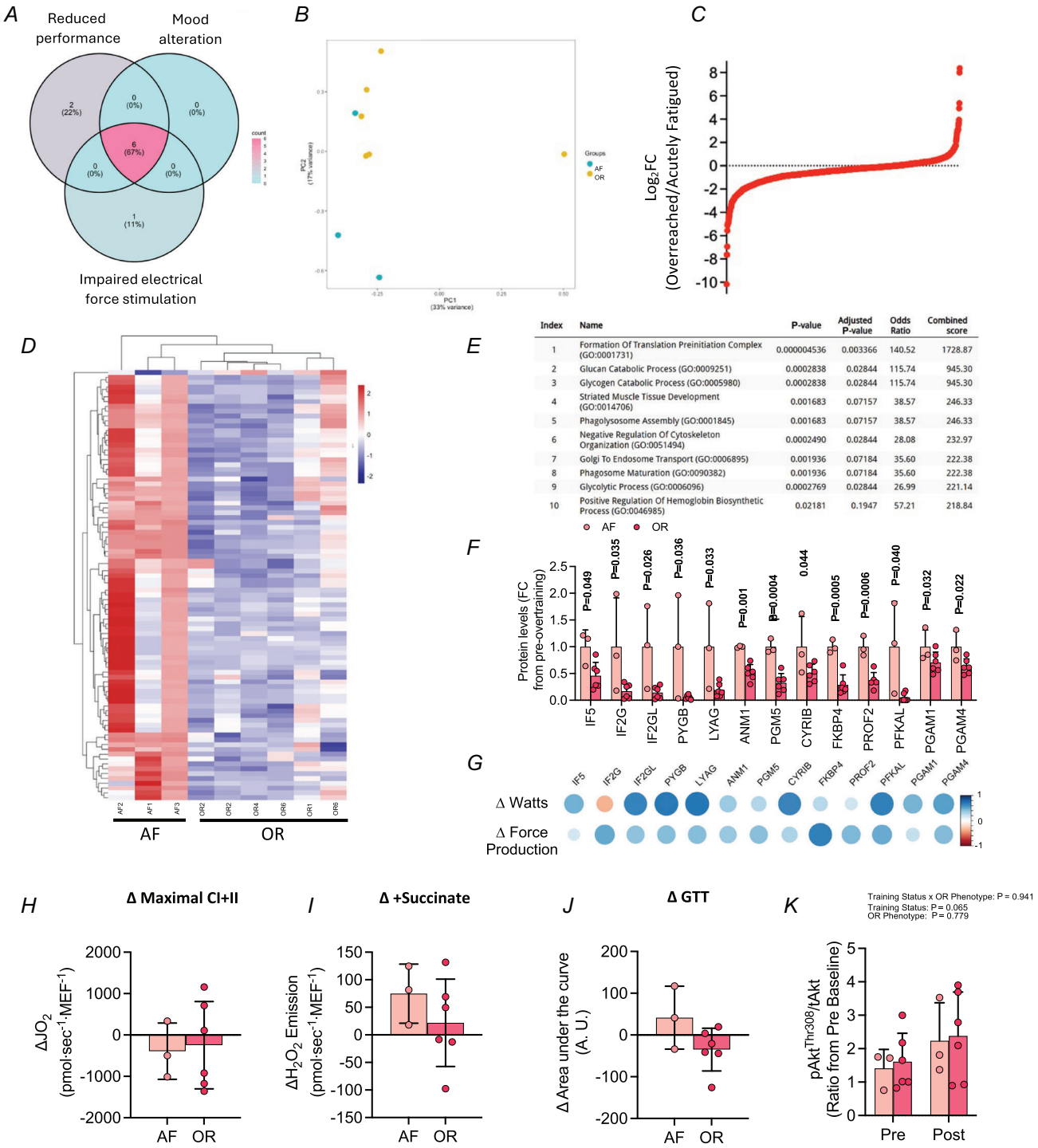

Figure 5. Overreaching elicits a unique molecular fingerprint in skeletal muscle
A, Venn diagram of individuals with reduced performance, mood alteration, and reduced force production in low-frequency. *B* and *C*, principal component analysis (*B*), and protein dynamic following overtraining (*C*), comparing overreached and acutely fatigued groups (n = 3 AF; 6 OR). *D*, heatmap of differentially regulated proteins after comparing overreached with acutely fatigued groups. *E*, enrichment analysis of biological processes using downregulated proteins in the overreached group. *F*, quantitative plot of enriched proteins in GO:0001731, GO:0005980, GO:0014706, GO:0051494 and GO:0006096. *G*, correlation analysis between differentially expressed proteins and performance metrics comparing overreached with acutely fatigued groups. *H* and *I*, changes in maximal mitochondrial respiration (*H*) as well as changes in succinate-driven H_2O_2 emission (*I*). *J*, changes in glucose tolerance test area under the curve. *K*, changes in muscle threonine Akt phosphorylation induced by acute glucose ingestion. Data expressed as means ± SD. Data met the assumption of normality as assessed by

the Shapiro–Wilk test were analysed using an unpaired, two-tailed Student's *t*-test (*H–K*). Bolded *P*-values are indicated for comparisons with a *P*-value of < 0.05. AF, acutely fatigued; ANM1, annexin A1; Akt, protein kinase b; CYRIB, CYFIP-related Rac1 interactor B; FKBP4, peptidyl-prolyl cis-trans isomerase FKBP4; GTT, glucose tolerance test; IF2G, interferon alpha-inducible protein 27-family member; IF2GL, interferon alpha-inducible protein 27-like protein 2; IF5, interferon-induced protein 35; LYAG, lysozyme g-like protein; MEF, mitochondrial enrichment factor; OR, Overreached; PFKAL, ATP-dependent 6-phosphofructokinase, liver type; PGAM1, phosphoglycerate mutase 1; PGAM4, probable phosphoglycerate mutase 4; PGM5, phosphoglucomutase-lik protein 5; PROF2, profilin-2; PGYB, glycogen phosphorylase, brain form

regulated by the exercise training protocol (Fig. 1*A*). Our analysis identified 89 differentially expressed proteins ($P < 0.05$) between groups, where the vast majority (i.e., 87) were downregulated in overreached participants compared to acutely fatigued participants (Fig. 5*D*). Enrichment analysis of these downregulated proteins revealed significant impacts on biological processes including 'formation of translation preinitiation complex' (GO:0001731, $P = 0.003$), 'glycogen catabolic process' (GO:0005980, $P = 0.028$), 'striated muscle tissue development' (GO:0014706, $P = 0.072$), 'negative regulation of cytoskeleton organization' (GO:0051494, $P = 0.028$) and 'glycolytic process' (GO:0006096, $P = 0.028$) (Fig. 5*E*). Notably, while exercise training upregulated these proteins in both groups, the overreached group had a blunted response compared to acutely fatigued group. Specifically, proteins involved in protein synthesis (i.e., IF5, $P = 0.049$; IF2G, $P = 0.035$; IF2GL, $P = 0.026$), carbohydrate metabolism (i.e., PYGB, $P = 0.036$; LYAG, $P = 0.033$; PGM5, $P = 0.004$; FKBP4, $P = 0.0005$; PFKL, $P = 0.040$; PGAM1, $P = 0.032$; and PGAM4, $P = 0.022$) (definition of abbreviation are defined in Fig 5 description), epigenetic programme and chromatin accessibility (i.e., ANM1, $P = 0.001$) and cytoskeletal remodelling (i.e., CYRIB, $P = 0.044$; PROF2, $P = 0.0006$) (Fig. 5*F*) suggesting a molecular mechanism underlying the impaired performance following the overtraining protocol. We next correlated the changes in performance (i.e., variation in watts produced during time trial test) (Coates et al., 2024) and in force production upon low-frequency (10 Hz) electrical stimulation of the quadriceps (Roussel et al., 2024) with the differentially expressed proteins enriched in the pathway analysis (Fig. 5*E*,*F*). Although reduction in electrical stimulated force-production was only significantly correlated with IF2GL, PYGB, LYAG, CYRIB and PFKAL ($r = 0.302$, 0.327, 0.321, 0.313 and 0.397, respectively), the strength of the relationship between them was medium/weak (Fig. 5*G*, $r < 0.4$). However, variation of performance positively correlated with proteins differentially expressed (IF2G, $r = 0.660$; PYGB, $r = 0.702$; LYAG, $r = 0.713$; CYRIB, $r = 0.650$; PFKAL, $r = 0.674$; PGAM1, $r = 0.462$; PGAM4, $r = 0.541$; all $P < 0.05$) in overreached/acutely fatigued individuals.

Given that mitochondrial dysfunction and impairments in glucose homeostasis were not observed following overtraining, we reassessed our mitochondrial phenotypic characterization dataset as well as our glucose-stimulated Akt-phosphorylation to determine inter-individual variability in response to overreaching. The change in maximal mitochondrial respiratory capacity and ROS production was similar between acutely fatigued and overreached (Fig. 5*H* and *I*, $P = 0.837$ and $P = 0.228$, respectively). Moreover, the blood glucose area under the curve remained unchanged (Fig. 5*J*, $P = 0.111$) and the improvement in insulin signalling ($pAkt^{Thr308}$/tAkt) within skeletal muscle following overtraining was preserved in those individuals defined as overreached (Fig. 5*K*, Training status × Overreached (OR) phenotype, $P = 0.941$; Training status, $P = 0.065$; OR phenotype, $P = 0.779$). Collectively, these data demonstrate that overreaching status is associated with a distinct molecular signature, which may explain the physiological basis for reduced performance and increased susceptibility to overreaching in certain athletes; however, mitochondrial function and insulin signalling remain preserved despite variability in the responsivity of the individuals to overtraining.

Discussion

In this study, we demonstrate that overtraining in endurance athletes does not compromise mitochondrial bioenergetics or insulin signalling within skeletal muscle. Instead, we illustrate that overtraining promotes substantial proteomic adaptations in skeletal muscle, including increased mitochondrial content and respiratory capacity, and the abundance of proteins associated with lipid metabolism, antioxidants, and insulin signalling. Notably, these mitochondrial adaptations occurred independent of changes in the intrinsic mitochondrial respiratory response and coincided with enhanced insulin signalling following an oral glucose challenge. Importantly, we identified a distinct molecular signature in overreached compared to acutely fatigued athletes, whereby the increase in proteins related to translation initiation, glycogen metabolism and contractile architecture was blunted. Collectively, these data suggest a mechanistic basis for the impaired performance that is independent of alterations in skeletal muscle mitochondrial bioenergetics and insulin signalling.

Exercise-induced mitochondrial adaptations typically occur concurrently with improvements in metabolic flexibility (Dubé et al., 2014; Smith et al., 2018). Prior research in this cohort of participants demonstrated that overreaching reduced carbohydrate utilization during submaximal exercise (Coates et al., 2024), suggesting greater reliance on lipid oxidation following the overload training protocol. Our findings reveal that skeletal muscle not only maintained, but even enhanced, its ability to respond to an acute glucose challenge at rest. In contrast to the impaired glucose control observed in recreationally trained individuals by Flockhart et al. (2021), we found no differences in blood glucose tolerance or associated blood insulin concentrations following our overtraining protocol. This finding aligns with related work that included many of the same participants, which similarly demonstrated that glycaemic control remains unchanged following overtraining (Ranahan et al., 2025). While previous work assessed systemic glucose tolerance, we additionally examined insulin signalling directly within skeletal muscle and found heightened Akt phosphorylation following glucose ingestion, alongside upregulation of proteins involved in glucose uptake (SLC2A4/GLUT4, GYS, and HK1) and increases in signal transduction components. This maintenance of insulin sensitivity despite preferential fat oxidation during submaximal exercise has been mechanistically linked to enhanced mitochondrial function. In fact, previous research has established the relationship between Gibbs free energy of ATP hydrolysis and oxidative phosphorylation rate as a significant predictor of insulin sensitivity independent of aerobic capacity (Zapata Bustos et al., 2023).

Our results demonstrate a consistent increase in mitochondrial content throughout the overtraining period, evidenced by the increase in MEF. However, in contrast to previous reports in the literature on impaired mitochondrial function following overtraining, we observed an enhancement in overall oxidative capacity. This was accompanied by increased mitochondrial H_2O_2 emission, and a reduction in ADP sensitivity (increased apparent K_m). These adaptations are largely consistent with chronic endurance training adaptations whereby higher ADP K_m reflects enhanced mitochondrial respiratory capacity rather than dysfunction (Miotto & Holloway, 2019; Zoll et al., 2002). When normalizing respiration to MEF, intrinsic mitochondrial function remained largely unchanged, suggesting that the enhanced respiratory capacity resulted from quantitative rather than qualitative mitochondrial adaptations. One interpretation of these findings is that the sprint interval efforts incorporated into the training stimulus induced brief, transient mitochondrial stress, which is considered part of an adaptive remodelling process rather than a driver of lasting dysfunction (Botella et al., 2025). However, the persistent elevation in H_2O_2 production normalized to MEF in the presence of submaximal ADP deserves further consideration, as it potentially indicates intrinsic alterations in mitochondrial redox regulation during periods of overtraining. While others report decreased mitochondrial ROS and Nrf2 protein abundance, our findings suggest a different adaptive response in well-trained athletes, with upregulation of downstream Nrf2 target proteins (SOD1, CAT, GRPX, and PRDX6) possibly due to an increased H_2O_2 production. It is possible that mitochondrial calcium overload can trigger elevated ROS levels (Peng & Jou, 2010), while environments characterized by continuous mitochondrial stimulation naturally produce proportionally increased ROS as byproducts of elevated metabolic activity (Neurohr et al., 2021). Specifically, higher aerobic capacity correlated with increased oxidative damage and exhibits elevated rates of protein and ATP turnover (Neurohr et al., 2021). The increased nitrotyrosine levels provide further evidence of oxidative stress, indicating that despite upregulation of antioxidant defence, cellular redox balance remains perturbed during the overtraining phase. Nevertheless, the functional implications of this perturbation, whether ultimately adaptive or maladaptive, remain to be determined.

Based on psychophysiological criteria, we identified distinct adaptive responses between overreached and acutely fatigued athletes, whereby some athletes had the ability to tolerate the intensified training load without having all the symptoms of overreaching following the same training protocol. Our proteome analysis revealed subtle molecular distinctions suggesting an underlying signature of overreaching susceptibility. Specifically, blunted responses in key proteins suggest impaired anabolic, metabolic and contractile apparatus, potentially underpinning the reduced performance observed in overreached individuals. Notably, the mechanistic relevance of these protein changes is supported by strong correlations between specific differentially expressed proteins and performance decrements. While changes in force production showed only modest correlations with select proteins, time-trial performance demonstrated robust correlations with proteins involved in translation initiation, glycogen metabolism, contractile performance and glycolysis. These strong performance–protein relationships suggest that the blunted molecular adaptation in overreached athletes may contribute to impaired exercise capacity. However, it should be noted that these correlational analyses do not establish causality, and the relationships observed may reflect associations rather than direct mechanistic links. Nevertheless, mechanistic studies addressing the physiological role of these proteins in exercise adaptations need to be

performed. Despite this molecular signature, we did not observe a reduction in mitochondrial function nor insulin signalling, challenging the current notion that the beneficial effects of exercise training reach a plateau when excessive volume/intensity is performed (Flockhart et al., 2021; Liu et al., 2025).

While our findings provide novel insights into skeletal muscle adaptations during overtraining, several limitations warrant consideration. First, our cohort was predominantly males ($n = 7$) with only two female participants, precluding sex-stratified analyses. Thus, future studies with adequately powered female cohorts are needed to determine whether our findings generalize across sexes. We also acknowledge the relatively modest sample size in our exploratory comparison between over-reached ($n = 6$) and acutely fatigued ($n = 3$) participants, where the inherent unpredictability of individual responses to intensified training contributed to unequal group sizes. Given these preliminary findings, additional research with a larger sample size is of interest for future studies to draw specific conclusions between responders and non-responders to overtraining. Additionally, cycling was chosen as the exercise modality to elicit overreaching as it was the most practiced across all of the endurance athletes and was the least likely modality to elicit an overuse injury; however, we do not know whether the results would be the same if a different exercise modality was chosen. Finally, our insulin measurements during OGTT were limited to baseline and 30 min post-glucose ingestion, which may not capture the complete insulin response throughout the glucose excursion during the test. We have, however, matched insulin measurements with skeletal muscle biopsies, enabling us to parallel whole-body metabolic responses to insulin signalling within skeletal muscle. While this approach enabled examination of tissue-level insulin signalling, future studies would benefit from capturing the complete insulin response curve to more comprehensively assess the effects of overtraining on glucose homeostasis.

In summary, we conclude that overload training induces mitochondrial biogenesis without impairing mitochondrial bioenergetics or insulin signalling in skeletal muscle of highly trained athletes. In addition, a distinct proteome signature was found between individuals who were overreached and those who were not, suggesting a fundamental molecular basis for exercise training adaptation.

References

Axelrod, C. L., Fealy, C. E., Mulya, A., & Kirwan, J. P. (2019). Exercise training remodels human skeletal muscle mitochondrial fission and fusion machinery towards a pro-elongation phenotype. *Acta Physiologica*, **225**(4), e13216.

Botella, J., Perri, E., Caruana, N. J., López-Calcerrada, S., Brischigliaro, M., Jamnick, N. A., Oorschot, V., Saner, N. J., Díaz-Lara, J., Taylor, D. F., Garnham, A., Fernández-Vizarra, E., Ugalde, C., Ramm, G., Stroud, D. A., Lazarou, M., & Bishop, D. J. (2025). Sprint interval exercise disrupts mitochondrial ultrastructure driving a unique mitochondrial stress response and remodelling in men. *Nature Communications*, **17**, 71.

Cardinale, D. A., Gejl, K. D., Petersen, K. G., Nielsen, J., Ørtenblad, N., & Larsen, F. J. (2021). Short-term intensified training temporarily impairs mitochondrial respiratory capacity in elite endurance athletes. *Journal of Applied Physiology*, **131**(1), 388–400.

Coates, A. M., Thompson, K. M. A., Grigore, M. M., Baker, R. E., Pignanelli, C., Robertson, A. A., Frangos, S. M., Cheung, C. P., & Burr, J. F. (2024). Altered carbohydrate oxidation during exercise in overreached endurance athletes is applicable to training monitoring with continuous glucose monitors. *Scandinavian Journal of Medicine & Science in Sports*, **34**(1), e14551.

Coetsee, C., & Terblanche, E. (2017). The effect of three different exercise training modalities on cognitive and physical function in a healthy older population. *European Review of Aging and Physical Activity*, **14**, 13.

Dubé, J. J., Coen, P. M., DiStefano, G., Chacon, A. C., Helbling, N. L., Desimone, M. E., Stafanovic-Racic, M., Hames, K. C., Despines, A. A., Toledo, F. G. S., & Goodpaster, B. H. (2014). Effects of acute lipid overload on skeletal muscle insulin resistance, metabolic flexibility, and mitochondrial performance. *American Journal of Physiology-Endocrinology and Metabolism*, **307**(12), E1117–E1124.

Eijsvogels, T. M. H., Thompson, P. D., & Franklin, B. A. (2018). The "extreme exercise hypothesis": Recent findings and cardiovascular health implications. *Current Treatment Options in Cardiovascular Medicine*, **20**(10), 84.

Fisher-Wellman, K. H., & Neufer, P. D. (2012). Linking mitochondrial bioenergetics to insulin resistance via redox biology. *Trends in Endocrinology & Metabolism*, **23**(3), 142–153.

Flockhart, M., Nilsson, L. C., Tais, S., Ekblom, B., Apró, W., & Larsen, F. J. (2021). Excessive exercise training causes mitochondrial functional impairment and decreases glucose tolerance in healthy volunteers. *Cell Metabolism*, **33**(5), 957–970.e6.

Frangos, S. M., Brunetta, H. S., Wang, D., Jabile, M. J. T., Ma, D. W., Muller, W. J., Khursigara, C. M., Fisher-Wellman, K. H., Steinberg, G. R., & Holloway, G. P. (2025). Intrinsic bioenergetic adaptations compensate for reduced mitochondrial content in HER2-driven mammary tumors. *eLife*, **14**, RP104079.

Greggio, C., Jha, P., Kulkarni, S. S., Lagarrigue, S., Broskey, N. T., Boutant, M., Wang, X., Conde Alonso, S., Ofori, E., Auwerx, J., Cantó, C., & Amati, F. (2017). Enhanced Respiratory chain supercomplex formation in response to exercise in human skeletal muscle. *Cell Metabolism*, **25**(2), 301–311.

Holloszy, J. O. (1967). Biochemical adaptations in muscle. Effects of exercise on mitochondrial oxygen uptake and respiratory enzyme activity in skeletal muscle. *Journal of Biological Chemistry*, **242**(9), 2278–2282.

Holloway, G. P., Holwerda, A. M., Miotto, P. M., Dirks, M. L., Verdijk, L. B., & Van Loon, L. J. C. (2018). Age-associated impairments in mitochondrial ADP sensitivity contribute to redox stress in senescent Human skeletal muscle. *Cell Reports*, **22**(11), 2837–2848.

Hooper, S. L., & Mackinnon, L. T. (1995). Monitoring overtraining in athletes: Recommendations. *Sports Medicine*, **20**(5), 321–327.

Hoppeler, H., Lüthi, P., Claassen, H., Weibel, E. R., & Howald, H. (1973). The ultrastructure of the normal human skeletal muscle. *Pflugers Archiv: European Journal of Physiology*, **344**(3), 217–232.

Hurrle, S., & Hsu, W. H. (2017). The etiology of oxidative stress in insulin resistance. *Biomedical Journal*, **40**(5), 257–262.

Kanehisa, M., Sato, Y., Kawashima, M., Furumichi, M., & Tanabe, M. (2016). KEGG as a reference resource for gene and protein annotation. *Nucleic Acids Research*, **44**(D1), D457–D462.

Lavie, C. J., Arena, R., Swift, D. L., Johannsen, N. M., Sui, X., Lee, D., Earnest, C. P., Church, T. S., O'Keefe, J. H., Milani, R. V., & Blair, S. N. (2015). Exercise and the cardiovascular system: Clinical science and cardiovascular outcomes. *Circulation Research*, **117**(2), 207–219.

Liu, Y., Zhou, R., Guo, Y., Hu, B., Xie, L., An, Y., Wen, J., Liu, Z., Zhou, M., Kuang, W., Xiao, Y., Wang, M., Xie, G., Zhou, H., Lu, R., Peng, H., & Huang, Y. (2025). Muscle-derived small extracellular vesicles induce liver fibrosis during overtraining. *Cell Metabolism*, **37**(4), 824–841.e8.

Luciano, E., Carneiro, E., Carvalho, C., Carvalheira, J., Peres, S., Reis, M., Saad, M., Boschero, A., & Velloso, L. (2002). Endurance training improves responsiveness to insulin and modulates insulin signal transduction through the phosphatidylinositol 3-kinase/Akt-1 pathway. *European Journal of Endocrinology*, **147**(1), 149–157.

Ludzki, A., Paglialunga, S., Smith, B. K., Herbst, E. A. F., Allison, M. K., Heigenhauser, G. J., Neufer, P. D., & Holloway, G. P. (2015). Rapid repression of ADP transport by Palmitoyl-CoA is attenuated by exercise training in humans: A potential mechanism to decrease oxidative stress and improve skeletal muscle insulin signaling. *Diabetes*, **64**(8), 2769–2779.

McLaughlin, K. L., Hagen, J. T., Coalson, H. S., Nelson, M. A. M., Kew, K. A., Wooten, A. R., & Fisher-Wellman, K. H. (2020). Novel approach to quantify mitochondrial content and intrinsic bioenergetic efficiency across organs. *Scientific Reports*, **10**(1), 17599.

Meeusen, R., Duclos, M., Foster, C., Fry, A., Gleeson, M., Nieman, D., Raglin, J., Rietjens, G., Steinacker, J., & Urhausen, A. (2013). Prevention, diagnosis and treatment of the overtraining syndrome: Joint consensus statement of the European College of Sport Science (ECSS) and the American College of Sports Medicine (ACSM). *European Journal of Sport Science*, **13**(1), 1–24.

Meinild Lundby, A.-K., Jacobs, R. A., Gehrig, S., de Leur, J., Hauser, M., Bonne, T. C., Flück, D., Dandanell, S., Kirk, N., Kaech, A., Ziegler, U., Larsen, S., & Lundby, C. (2018). Exercise training increases skeletal muscle mitochondrial volume density by enlargement of existing mitochondria and not de novo biogenesis. *Acta Physiologica*, **222**(1), e12905.

Miotto, P. M., & Holloway, G. P. (2019). Exercise-induced reductions in mitochondrial ADP sensitivity contribute to the induction of gene expression and mitochondrial biogenesis through enhanced mitochondrial H_2O_2 emission. *Mitochondrion*, **46**, 116–122.

Miotto, P. M., LeBlanc, P. J., & Holloway, G. P. (2018). High-fat diet causes mitochondrial dysfunction as a result of impaired ADP sensitivity. *Diabetes*, **67**(11), 2199–2205.

Neurohr, J. M., Paulson, E. T., & Kinsey, S. T. (2021). A higher mitochondrial content is associated with greater oxidative damage, oxidative defenses, protein synthesis and ATP turnover in resting skeletal muscle. *Journal of Experimental Biology*, **224**(19), jeb242462.

Nielsen, J., Gejl, K. D., Hey-Mogensen, M., Holmberg, H., Suetta, C., Krustrup, P., Elemans, C. P. H., & Ørtenblad, N. (2017). Plasticity in mitochondrial cristae density allows metabolic capacity modulation in human skeletal muscle. *The Journal of Physiology*, **595**(9), 2839–2847.

Peng, T., & Jou, M. (2010). Oxidative stress caused by mitochondrial calcium overload. *Annals of the New York Academy of Sciences*, **1201**, 183–188.

Perry, C. G. R., Lally, J., Holloway, G. P., Heigenhauser, G. J. F., Bonen, A., & Spriet, L. L. (2010). Repeated transient mRNA bursts precede increases in transcriptional and mitochondrial proteins during training in human skeletal muscle: Molecular responses during mitochondrial biogenesis. *The Journal of Physiology*, **588**(Pt 23), 4795–4810.

Petrick, H. L., & Holloway, G. P. (2019). High intensity exercise inhibits carnitine palmitoyltransferase-I sensitivity to L -carnitine. *Biochemical Journal*, **476**, 547–558.

Rains, J. L., & Jain, S. K. (2011). Oxidative stress, insulin signaling, and diabetes. *Free Radical Biology and Medicine*, **50**(5), 567–575.

Ramos-Cabrer, P., Cabrera-Zubizarreta, A., Padro, D., Matute-González, M., Rodríguez-Antigüedad, A., & Matute, C. (2025). Reversible reduction in brain myelin content upon marathon running. *Nature Metabolism*, **7**, 697–703.

Ranahan, A. M., Pignanelli, C., Thompson, K. M. A., Burr, J. F., & Coates, A. M. (2025). Alterations in glycemic control and glucose tolerance following overtraining in endurance athletes. *Applied Physiology, Nutrition and Metabolism*, **50**, 1–10.

Rath, S., Sharma, R., Gupta, R., Ast, T., Chan, C., Durham, T. J., Goodman, R. P., Grabarek, Z., Haas, M. E., Hung, W. H. W., Joshi, P. R., Jourdain, A. A., Kim, S. H., Kotrys, A. V., Lam, S. S., McCoy, J. G., Meisel, J. D., Miranda, M., Panda, A., … Mootha, V. K. (2021). MitoCarta3.0: An updated mitochondrial proteome now with sub-organelle localization and pathway annotations. *Nucleic Acids Research*, **49**(D1), D1541–D1547.

Roussel, O. P., Pignanelli, C., Hubbard, E. F., Coates, A. M., Cheng, A. J., Burr, J. F., & Power, G. A. (2024). Effects of intensified training with insufficient recovery on joint level and single muscle fibre mechanical function: The role of myofibrillar Ca^{2+} sensitivity. *Applied Physiology, Nutrition and Metabolism*, **49**(12), 1646–1657.

Saltin, B., Lindgärde, F., Houston, M., Hörlin, R., Nygaard, E., & Gad, P. (1979). Physical training and glucose tolerance in middle-aged men with chemical diabetes. *Diabetes*, **28**(Suppl 1), 30–32.

Smith, B. K., Perry, C. G. R., Herbst, E. A. F., Ritchie, I. R., Beaudoin, M.-S., Smith, J. C., Neufer, P. D., Wright, D. C., & Holloway, G. P. (2013). Submaximal ADP-stimulated respiration is impaired in ZDF rats and recovered by resveratrol. *The Journal of Physiology*, **591**(Pt 23), 6089–6101.

Smith, R. L., Soeters, M. R., Wüst, R. C. I., & Houtkooper, R. H. (2018). Metabolic flexibility as an adaptation to energy resources and requirements in health and disease. *Endocrine Reviews*, **39**(4), 489–517.

Snow-Harter, C., Bouxsein, M. L., Lewis, B. T., Carter, D. R., & Marcus, R. (1992). Effects of resistance and endurance exercise on bone mineral status of young women: A randomized exercise intervention trial. *Journal of Bone and Mineral Research*, **7**(7), 761–769.

Symons, I. K., Bruce, L., & Main, L. C. (2023). Impact of overtraining on cognitive function in endurance athletes: A systematic review. *Sports Medicine – Open*, **9**(1), 69.

Xie, Z., Bailey, A., Kuleshov, M. V., Clarke, D. J. B., Evangelista, J. E., Jenkins, S. L., Lachmann, A., Wojciechowicz, M. L., Kropiwnicki, E., Jagodnik, K. M., Jeon, M., & Ma'ayan, A. (2021). Gene set knowledge discovery with Enrichr. *Current Protocols*, **1**(3), e90.

Zapata Bustos, R., Coletta, D. K., Galons, J.-P., Davidson, L. B., Langlais, P. R., Funk, J. L., Willis, W. T., & Mandarino, L. J. (2023). Nonequilibrium thermodynamics and mitochondrial protein content predict insulin sensitivity and fuel selection during exercise in human skeletal muscle. *Frontiers in Physiology*, **14**, 1208186.

Zhang, M., Jia, J., Yang, Y., Zhang, L., & Wang, X. (2023). Effects of exercise interventions on cognitive functions in healthy populations: A systematic review and meta-analysis. *Ageing Research Reviews*, **92**, 102116.

Zoll, J., Sanchez, H., N'Guessan, B., Ribera, F., Lampert, E., Bigard, X., Serrurier, B., Fortin, D., Geny, B., Veksler, V., Ventura-Clapier, R., & Mettauer, B. (2002). Physical activity changes the regulation of mitochondrial respiration in human skeletal muscle. *The Journal of Physiology*, **543**(Pt 1), 191–200.

Additional information

Data availability statement

The data that support the findings of this study are available from the corresponding author upon reasonable request.

Competing interests

The authors declare they have no competing interests.

Author contributions

G.J.D., H.S.B., A.M.C., J.F.B. and G.P.H. conceived and designed the research. G.J.D., H.S.B., P.A.B., A.M.C., C.P. and F.A.R. performed data collection, and analysis. G.J.D., H.S.B. and G.P.H. drafted the manuscript. Revisions were performed by all authors. All authors have read and approved the final version of this manuscripft and agree to be accountable for all aspects of the work in ensuring that questions related to the accuracy or integrity of any part of the work are appropriately investigated and resolved. All persons designated as authors qualify for authorship, and all those who qualify for authorship are listed.

Funding

This research was supported by the Natural Sciences and Engineering Research Council of Canada (NSERC).

Keywords

glucose, metabolism, overtraining, proteome, skeletal muscle

Supporting information

Additional supporting information can be found online in the Supporting Information section at the end of the HTML view of the article. Supporting information files available:

Peer Review History
Table S1
Table S2